Available online at www.sciencedirect.com
SCIENCE DIRECT®
Applied Surface Science 222 (2004) 365–373
applied surface science
www.elsevier.com/locate/apsusc

The early stages of silicon surface damage induced by pulsed CO_2 laser radiation: an AFM study

D.-Q. Yang[a,b], E. Sacher[a,b,*], M. Meunier[a,b]

[a]*Laboratoire de Procédés Laser, Groupe des Couches Minces, C.P. 6079, succursale Centre-Ville, Montreal, Que., Canada H3C 3A7*
[b]*Département de Génie Physique, École Polytechnique, C.P. 6079, succursale Centre-Ville, Montreal, Que., Canada H3C 3A7*

Received 9 July 2003; received in revised form 3 September 2003; accepted 3 September 2003

Abstract

The early stages of the surface microstructural modification of silicon, induced by single pulses of CO_2 laser irradiation ($\lambda = 10.6$ μm), have been studied, in both vacuum and air, by contact mode AFM. The laser pulse was found to be absorbed at the front surface of the sample, facing the laser; this was shown to be due to the presence of native oxide, which absorbs at this wavelength. We found that this absorption of energy caused the stress-induced formation of vertically oriented, square-shaped fragments, 400–700 nm in length, often with short branches, that form a wall around the impact site; they oriented toward the plane of the sample with distance from the impact site, aligning more in the electric field direction of the pulse. In addition, electrically charged, branched fragments were redeposited at the outer extremities of the pulse site.

Keywords: CO_2 laser; Silicon; Surface structure; Surface morphology

1. Introduction

The microstructural modifications of solid surfaces by pulsed lasers have received much attention in recent years [1–8], due the ability of this process to produce new, unexpected patterns that may have potential applications to photonics [9], microfabrication [10–15], electronics [16], and magnetic field production [17]. Silicon, in particular, due its important role in microelectronics, has been widely used to produce such surface patterns. As examples [3,4,7,10,15,18–21], it has been possible to create ripples, microcolumns and microcolumn arrays, microcones, as well as the long-range ordering of Si nanoparticles, in both air and SF_6. This has been accomplished through the irradiation of uncleaned (native oxide-coated) Si wafer surfaces by KrF ($\lambda = 248$ nm), Cu vapor ($\lambda = 510.6$ nm), and Nd:YAG ($\lambda = 532$ nm) pulsed lasers, etc. Huang et al. [8], using a Nd:YAG pulsed laser, coupled with atomic force microscopy (AFM), produced nanopatterns, such as arrays of pits and multiple lines, with lateral dimensions between 10 and 50 nm and depths of 2.5–21 nm, on metallic Au and Cu layers on Si substrates.

Surprisingly, despite the fact that Si is transparent at the CO_2 laser IR wavelength of 10.6 μm (corresponding to a photon energy of 0.12 eV), recent results from several authors [9,14,22] showed that structures were, in fact, produced. For example, Wang et al. [14] reported that they were able to controllably create periodic structures on the Si surface, at low CO_2 power densities, when the wafer back side (facing away from

* Corresponding author. Tel.: +1-514-340-4711x4858; fax: +1-514-340-3218.
E-mail address: edward.sacher@polymtl.ca (E. Sacher).

0169-4332/$ – see front matter © 2003 Elsevier B.V. All rights reserved.
doi:10.1016/j.apsusc.2003.09.025

the laser) was coated with a thin Au or similar layer. In contradistinction, Trtica and Gaković [22], using higher laser energy densities, showed that periodic ripples could be produced by the CO_2 laser without a metallic layer coating on the wafer back side. Further, Kabashin and Meunier [9] showed that a nanoporous Si surface could be produced by the CO_2 laser irradiation of a commercial silicon wafer, which then demonstrated strong room temperature photoluminescence in the visible light region.

Because the Si band gap energy, 1.12 eV at room temperature (corresponding to a photon wavelength 1.11 μm), is much higher than that of a CO_2 laser photon (0.12 eV), it is assumed that a CO_2 laser does not have enough energy to excite an electron from the valence band of Si into the conduction band. The optical absorption that produced the laser damage is then attributed [14,22] to some deep energy states within the forbidden gap, created by impurities, surface and/or bulk defects.

The photoluminescent behavior of porous Si has been associated with microstructures and surface chemistry [9,23], which depends [23] on the radiation conditions and the ambient gas species. Because of this uncertainty, and our interest in Si surface structure as influenced by lasers, we felt it necessary to better understand the mechanism of surface structural modification caused by the CO_2 laser, which is why we initially undertook this study. We were, therefore, pleasantly surprised to find that the recent publication of Trtica and Gaković [22] explored the same pulsed CO_2 laser irradiation of Si we were considering. While our results differ, in that we explore the results of single pulses (later stages will be considered in a subsequent publication [23]), we support many of their findings while obtaining a deeper understanding of the energy transfer mechanism. Our papers should be considered complementary.

2. Experimental

The experiments were carried by a Lumonics pulsed TEA CO_2 laser (10.6 μm = 943 cm^{-1}) with a pulse energy of ∼1 J, a pulse duration of 1 μs FWHM, a repetition rate of 3 Hz and a radiation intensity of $\sim 5 \times 10^7$ W/cm. The laser was not intentionally polarized but was focused by a Fresnel lens whose focal length was about 15 cm, and its position was held constant. The shape of the beam is an ellipse whose intensity is Gaussian in form. The dimensions of the ellipse thus depend on the method of detection: this is because the detector (in our case, a Si wafer) shows only that portion of the center of the beam whose energy density is sufficiently high to cause pits in the substrate. In our case, the vast majority of pits had a major axis of ∼150 μm and a minor axis of ∼100 μm, although occasional pits were smaller (∼100 μm × 60 μm). The ellipses were invariably aligned in the same direction.

The Si wafers used were both n- and p-type, with resistivities of 0.01–10 Ω cm. Because Si wafers whose native oxide has been cleaned off recontaminate quickly on exposure to air, no attempt was made to remove the native oxide, as with much of the literature on Si; instead, the wafers were cleaned with organic solvents, after being broken but prior to use, and then permitted to dry. This is the procedure followed by other workers [3,4,7,10,15,18–21].

The wafers were cut into 1 cm × 1 cm pieces, with no debris evident by AFM on cleaning. These samples were subjected to laser irradiation in either air or vacuum. Samples were held vertically, perpendicular to the laser beam to avoid surface recontamination by debris; both n- and p-type samples gave the same results, and no distinction could be made between irradiation in air or vacuum at this small number of pulses.

Microscopic observations of the Si surfaces, after ∼3 laser pulses, showed individual impact craters (pits), invariably formed at the front sample surface, facing the laser, and equal to the number of pulses, differing in position although the laser was not moved. They were randomly distributed on the surface, although confined to an ultimate area of ∼0.6 mm × 1.8 mm. This is seen in Fig. 1, which contains the accumulated pits for several thousand continuous pulses; note that surface melting has occurred, obscuring the pits. This gives an average of about 5×10^7 W/cm^2 of radiation intensity over the whole area. The irradiation was carried in a chamber that could be evacuated to less than 10^{-4} Torr or backfilled, with any of several gases, to atmospheric pressure. The air environment to which the sample was exposed was at 22 °C and 30% relative humidity.

Analysis by atomic force microscopy (AFM) was carried out immediately following laser irradiation.

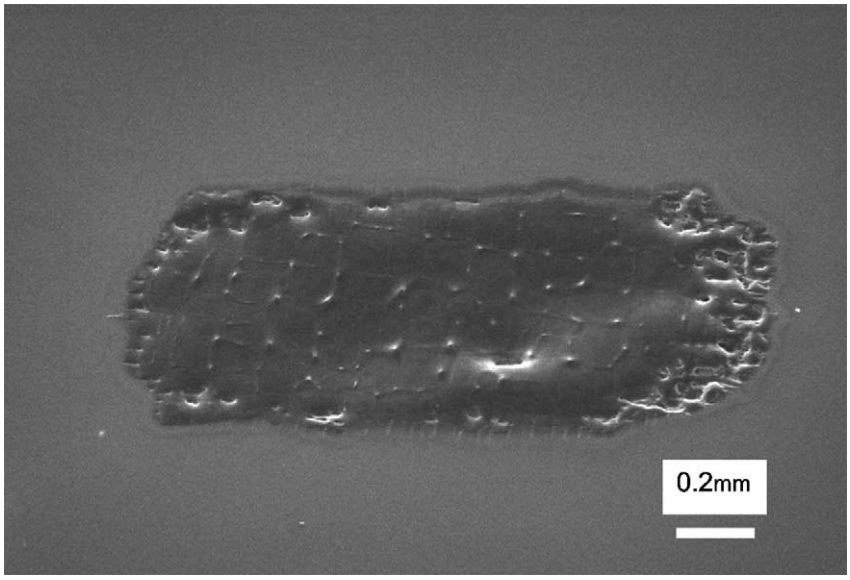

Fig. 1. SEM image of the area of laser irradiation after 1800 pulses in vacuum. The structures evident in the image will be discussed in a subsequent paper [23], on prolonged irradiation.

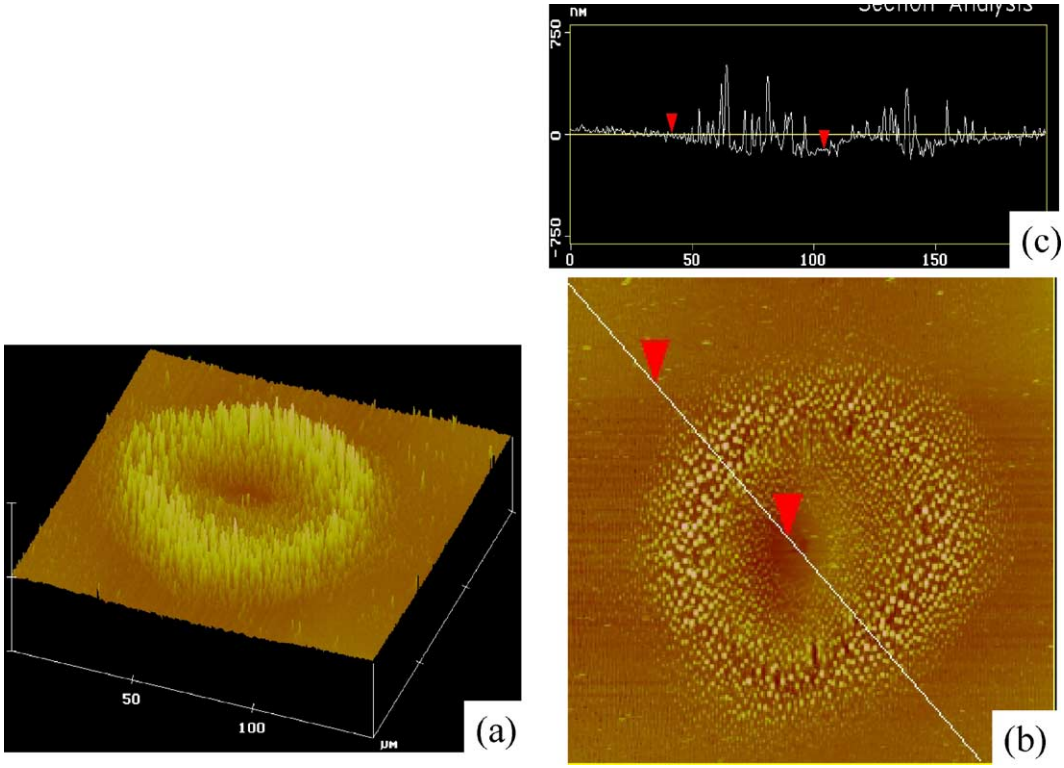

Fig. 2. AFM image of (a) the area immediately surrounding the impact pit produced in air; (b) vertical rod alignment; (c) profile. The images are 150 µm on a side.

Contact mode AFM was performed on a Digital Multimode Scanning Probe Microscope, using standard Si_3N_4 cantilevers in ambient air. These cantilevers had spring constants of 0.5 N/m, a typical tip radius of ~10–20 nm and a tip half-angle of 35°. The tip scanning rate was 2 Hz, and 512 lines were used per image.

3. Results

Occasional laser pulses were found to be somewhat lower in energy than the others, as suggested by the size of the impact crater (indicating an occasional energy variation). None of the pits produced by the unscanned beam overlapped exactly but varied slightly in position, being confined to a rectangle 0.6 mm × 1.8 mm, as mentioned earlier. This phenomenon may be related to the pulse-to-pulse energy variation. These variations permitted the observation of the effects of single pulses.

We noticed the formation of a momentary plasma on laser irradiation in air, while no plasma was observed in vacuum. As we shall show in a subsequent paper [23], the plasma state is strongly dependent on the gas species.

The inspection of many AFM images showed some variation among images but little overall difference between single pulse irradiation in air (a typical image is seen in Fig. 2) and in vacuum (Fig. 3), although, as we shall report in a future article [23], a large number of pulses, leading to the observation of a sustained plasma, showed substantial differences between the two; further, there appeared to be more partial pit overlap in vacuum, as shown in Fig. 3, which may not be real, given the limited number (20) of samples studied in vacuum.

Based on over 100 observations, the following characteristics were observed:

- The pit was always observed at the front (polished) substrate surface, facing the laser, never below the

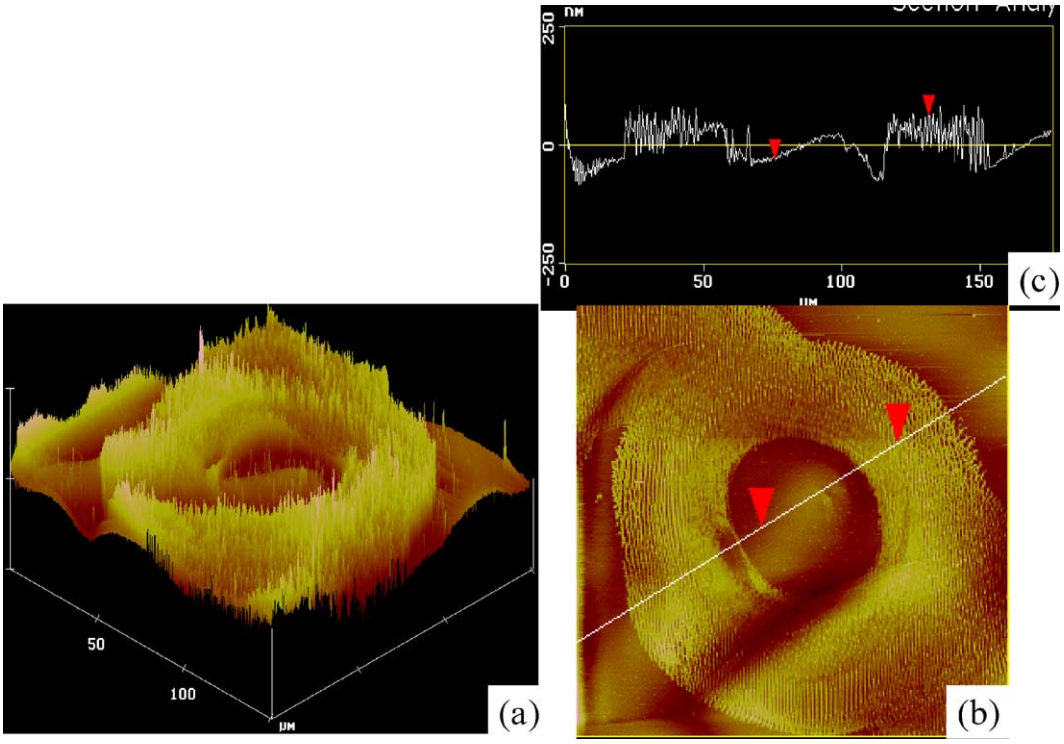

Fig. 3. AFM image of (a) the area immediately surrounding the impact pit produced in vacuum; (b) vertical rod alignment; (c) profile. The images are 150 μm on a side.

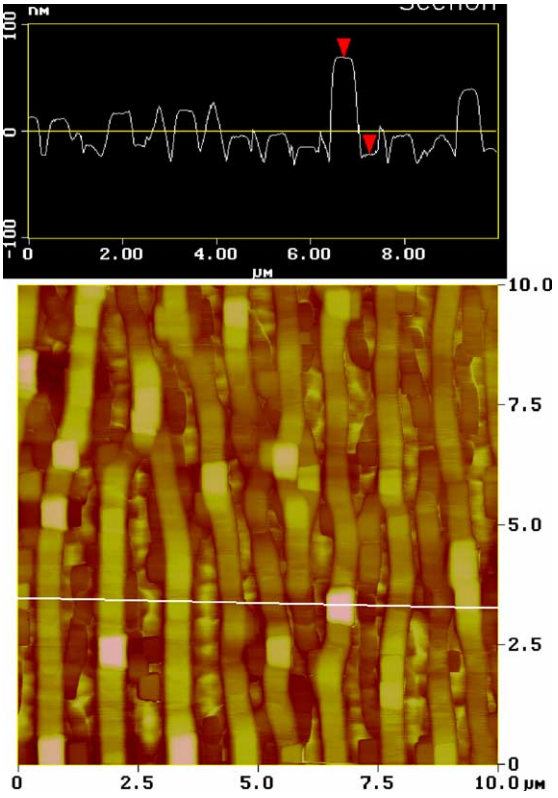

Fig. 4. AFM image at a distance from the simpact pit produced in air, with horizontal, branched rods. The image is 10 μm on a side.

surface or at the back (unpolished) side of the sample.

- The area immediately surrounding the pit was characterized by the presence of aligned, square-shaped rods, 400–700 nm in length, oriented perpendicular to the sample, with separations between rods of 200–700 nm.
- As the distance from the pit increased, the rods oriented more toward the horizontal, aligned in the direction of the major axis of the laser, and contained short, square branches (Fig. 4).
- Some material lost from the center of the pit was redeposited at the outer periphery of the impact area (Fig. 5), and was characterized by crosshatched sections, also square-shaped.
- The occasional lower energy laser pulses (as surmised from the smaller pit) were characterized by nonlinear (wiggly) square-shaped rods, found even in the center of the pit, and oriented more towards the plane of the sample, in the electrical field direction (Fig. 6).

4. Discussion

Although undoped Si is transparent at the energy of the CO_2 laser, this transparency is attenuated by the uniform distribution of dopants in both the n- and p-type Si samples used here. While this, and other, phenomena have been suggested [22,24,25] as possible reasons for the absorption of laser energy by Si, such explanations are untenable, given the fact that we have shown that the laser energy is absorbed uniquely at the front sample surface. The defect causing such absorption exists exclusively there.

One defect capable of causing laser absorption at the substrate surface is surface contamination, sometimes called ‘‘native oxide’’, a contamination so pervasive that the microelectronics industry must remove it at almost every step of the manufacturing process. Our studies of this contamination phenomenon [26,27] have shown that even the best cleaning efforts at our disposal result in surfaces that recontaminate within an hour or less. A photoacoustic IR spectrum of this native oxide, in Fig. 7, shows that this ‘‘oxide’’ contains –OH, $–CH_n$, $\diagdown\!\!\diagup C{=}O$, –Si–O–C– and –Si–O–Si–. The associated XPS spectrum, not shown, indicates that both the C 1s and Si 2p spectra contain partially, as well as fully, oxidized components. As Fig. 7 indicates, there is significant absorption at 943 cm^{-1} (note that this is a photoacoustic spectrum, which means that there is a signal only when there is absorption).

The contribution of the native oxide to surface damage was confirmed in the following way: we removed the native oxide by solution cleaning, which, as previously described [26,27], kept the surface uncontaminated for an hour or so. The surface damage caused by single laser pulses was followed as a function of atmospheric exposure time; the shortest time feasible, due to sample drying and mounting, was ~30 min, at which time the extent of pitting was invisible to the eye as well as by AFM. However, the pitting increased with air exposure over the next day or so.

Another possible defect, the presence of free radicals, appears not to contribute to pit formation, since we observe identical surface patterns after 3 keV Ar^+

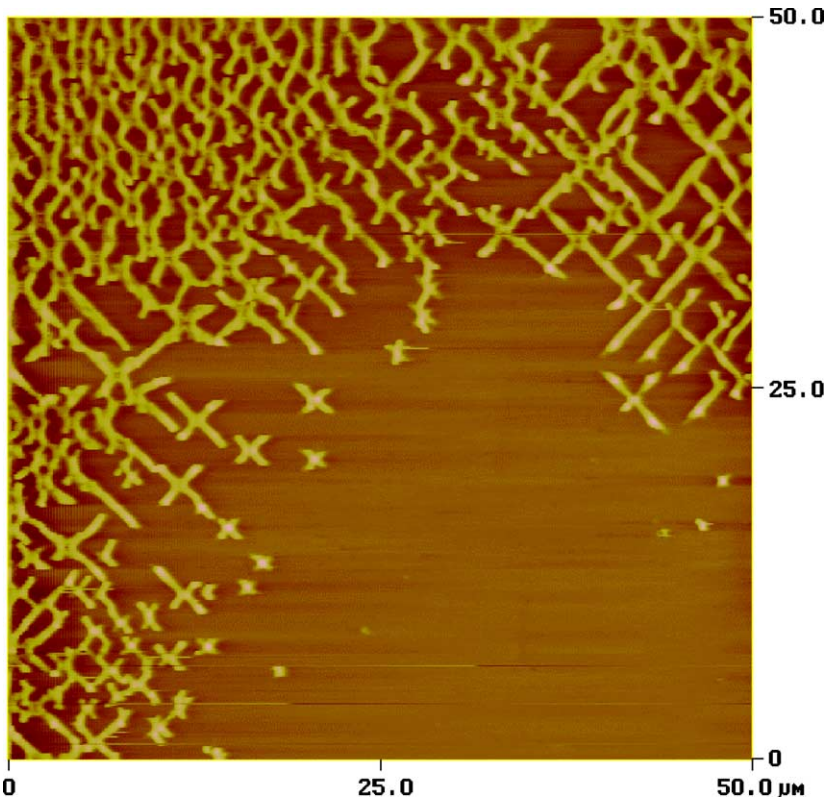

Fig. 5. AFM image away from the pit produced in air, with redeposited material.

beam irradiation prior to CO_2 laser irradiation. Such irradiation penetrates the surface, as shown by a SRIM simulation [28], fragmenting bonds in the bulk. Some of these fragments react with the atmosphere while others remain, below the surface, as free radicals; their presence did not cause subsurface laser damage.

The absence of any difference in pit morphology, between those formed in air and vacuum, is due to the absence of a sustained plasma. Such sustained plasmas are seen only on prolonged irradiation [23] in gaseous atmospheres (air, O_2, N_2, etc.), and their presence leads to different structures for different gases, indicating plasma–surface interactions. This will be discussed in a future paper [23].

The profile of the pit and the surrounding area Figs. 2c and 3c) resemble the mathematical solution to the Boussinesq problem for an axisymmentric force normal to the plane of a semi-infinite solid [29–31]. For an axisymmetric force (the laser radiation) of radius, r, Boussinesq determined that the force distribution in the semi-infinite solid (the Si substrate) is a minimum at the center of the applied force, rising exponentially as r is approached. If this simile is, indeed, correct, the deformation behavior in the radiation impact area (i.e. the pit and its immediate surroundings) may well be explained through the application of contact mechanics in a model that is capable of calculating the contact force; such a model should consider the extents of energy reflection and absorption. Without such an understanding, it is difficult to suggest the extent of Si melting and why it should form square-shaped rods. Indeed, Figs. 2 and 3 (and others not shown) suggest that melting may have occurred in the center of the pit.

The orientation of the rods beyond the impact area, invariably in the direction of the major axis of the ellipse, indicates a different mechanism. Such orientation was seen by Trtica and Gaković [22] for Si filaments (laser-induced periodic surface structure, LIPSS [32,33]), although for several hundred pulses

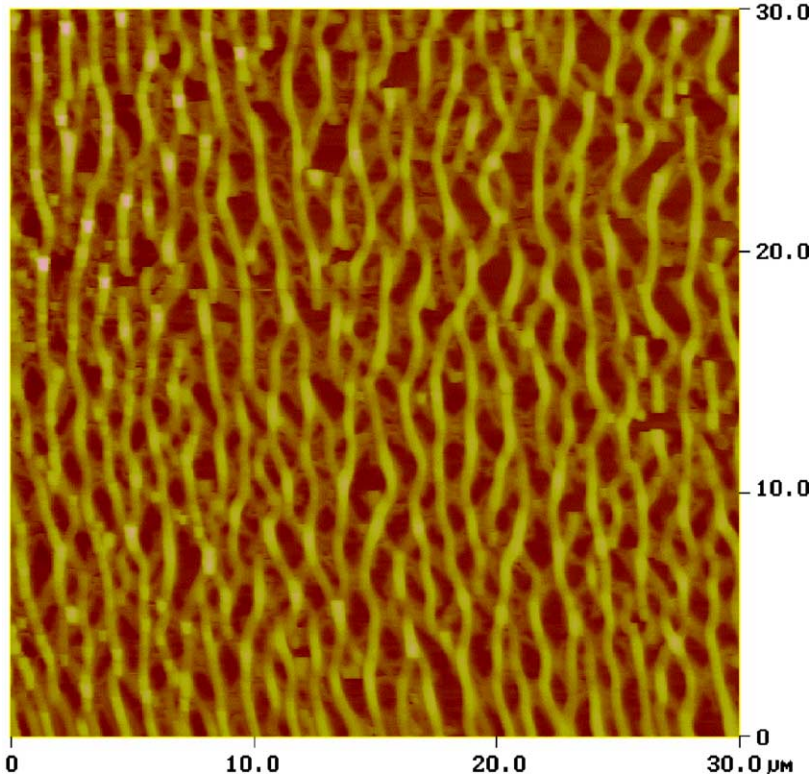

Fig. 6. AFM image of lower energy impact produced in air, with nonlinear rods.

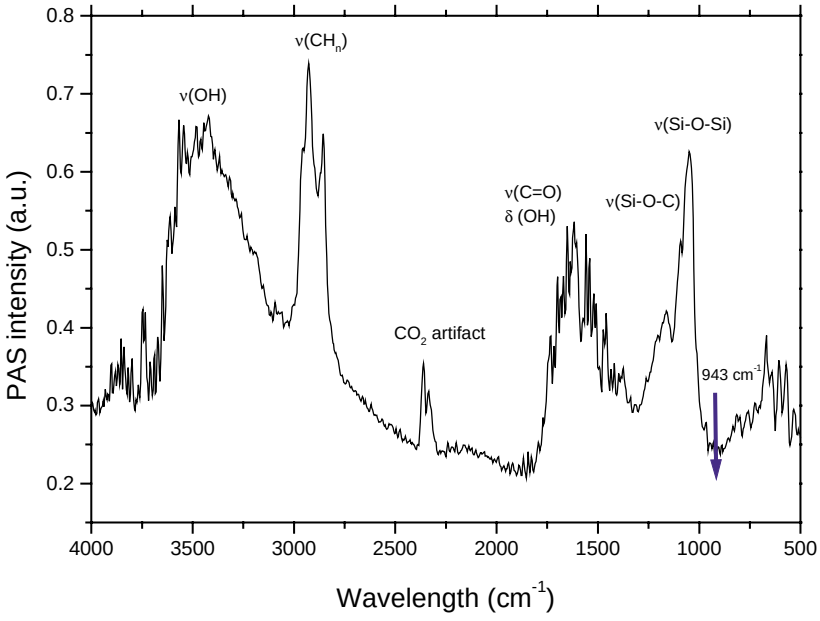

Fig. 7. Photoacoustic FTIR spectrum of a Si wafer covered with native oxide.

of CO_2 irradiation rather than the single pulses used here. Clearly, this argues for a distribution of electrical charges, along the rod, forming a dipole that can be oriented in an electrical field. Since the Si is doped to high conductivity, it would be expected that any charge distribution would be neutralized, leaving, at most, a single excess charge incapable of causing orientation. The fact that this does not happen indicates that the charges are distributed in the ''natural oxide'' insulating layer discussed previously. While we could find no information on electric fields in the beam, no other reason for the orientation seems to be evident.

The LIPSS mechanism indicates [34] that ripples should be produced with a period, l, given, at normal incidence, by

$$l = \frac{\lambda}{n}$$

where λ is the laser wavelength and n the refractive index of the substrate. The square rods formed in the present case are substantially smaller (400–700 nm) than the LIPSS prediction of $\sim$3 μm. Thus, it is highly improbable that the structures formed here follow the LIPSS mechanism. On the other hand, as we shall show in a subsequent paper on the later stages of Si surface irradiation by a CO_2 laser [23] in O_2, the structures formed in that case do, indeed, correspond to the LIPSS mechanism.

Another phenomenon arguing for electrostatic charging is the redeposition of some of the material ablated from the pit, beyond the impact area, unexpected in a vertical sample in the absence of electrical charges. The reason for the hatched forms in presently unknown.

5. Conclusions

We have observed the surface microstructural modification of Si at the early stages of CO_2 laser irradiation. Contact mode AFM has shown the contributions of several phenomena, including laser energy transfer at the front sample surface, and the production of charged structures. The presence of Si surface contamination has been shown to be necessary for the production of these structures, which may have application in field emission and photonics.

Acknowledgements

We thank the Natural Sciences and Engineering Research Council of Canada for funding.

References

[1] T. Yoshida, S. Takeyamada, K. Mutoh, Appl. Phys. Lett. 68 (1996) 1772.
[2] Y.F. Lu, J.J. Yu, W.K. Choi, Jpn. J. Appl. Phys. 37 (1998) 3471.
[3] A.J. Pedraza, J.D. Fowlkes, D.H. Lowndes, Appl. Phys. Lett. 74 (1999) 2322.
[4] X.Y. Chen, Z.G. Liu, Appl. Phys. A 69 (1999) S523.
[5] M. Csete, O. Marrti, Z. Bor, Appl. Phys. A 73 (2001) 521.
[6] J.J. Yu, J.Y. Zhang, I.W. Boyd, Y.F. Lu, Appl. Phys. A 72 (2001) 35.
[7] J.D. Fowlkes, A.J. Pedraza, D.A. Blom, H.M. Meyer III, Appl. Phys. Lett. 80 (2002) 3799.
[8] S.M. Huang, M.H. Hong, B.S. Luk'yanchuk, Y.F. Lu, W.D. Song, T.C. Chong, J. Vac. Sci. Technol. B 20 (2002) 1118.
[9] A. Kabashin, M. Meunier, Appl. Surf. Sci. 186 (2002) 578.
[10] D.H. Lowndes, J.D. Fowlkes, A.J. Pedraza, Appl. Surf. Sci. 154–155 (2000) 647.
[11] Y.F. Lu, B. Hu, Z.H. Mai, W.J. Wang, W.-K. Chim, T.C. Chong, Jpn. J. Appl. Phys. 40 (2001) 4395.
[12] J. Bonse, S. Baudach, J. Krüger, W. Kautek, M. Lenzner, Appl. Phys. A 74 (2002) 19.
[13] X.Y. Chen, Y.F. Lu, B.J. Cho, Y.P. Zeng, J.N. Zeng, Y.H. Wu, Appl. Phys. Lett. 81 (2002) 1344.
[14] W.J. Wang, Y.F. Lu, C.W. An, M.H. Hong, T.C. Chong, Appl. Surf. Sci. 186 (2002) 594.
[15] A.J. Pedraza, J.D. Fowlkes, D.H. Lowndes, Appl. Phys. A 69 (1999) S731.
[16] V.V. Zhirnov, E.I. Givargizov, P.S. Piekanov, J. Vac. Sci. Technol. B 13 (1995) 418;
A.V. Karabutov, V.D. Frolov, E.N. Loubnin, A.V. Simakin, G.A. Shafeev, Appl. Phys. A 76 (2003) 413.
[17] J.J. Yu, J.Y. Zhang, I.W. Boyd, Appl. Phys. A 72 (2001) 687.
[18] F. Sánchez, J.L. Morenza, R. Aguiar, J.C. Delgado, M. Varela, Appl. Phys. Lett. 69 (1996) 620;
F. Sánchez, J.L. Morenza, R. Aguiar, J.C. Delgado, M. Varela, Appl. Phys. A 66 (1998) 83.
[19] T.H. Her, R.F. Finlay, C. Wu, S. Deliwala, E. Mazur, Appl. Phys. Lett. 73 (1998) 383;
T.H. Her, R.F. Finlay, C. Wu, S. Deliwala, E. Mazur, Appl. Phys. A 70 (2000) 383.
[20] C. Wu, C.H. Crouch, L. Zhao, J.E. Carey, R. Younkin, J.A. Levinson, E. Mazur, R.M. Farelli, P. Gothoskar, A. Karger, Appl. Phys. Lett. 78 (2001) 1850.
[21] S.I. Dolgaev, S.V. Lavrischev, A.A. Lyalin, A.V. Simakin, V.V. Voronov, G.A. Shafeev, Appl. Phys. A 73 (2001) 177.
[22] M.S. Trtica, B.M. Gaković, Appl. Surf. Sci. 205 (2003) 336.

[23] D.-Q. Yang, A. Kabashin, V.G. Pilon-Marien, E. Sacher, M. Meunier, submitted for publication.
[24] T. Sakka, S. Akiba, A. Kuroyanagi, Y.H. Ogata, M. Mabuchi, Plasma Ions 1 (1998) 23;
T. Sakka, S. Akiba, A. Kuroyanagi, Y.H. Ogata, M. Mabuchi, Appl. Surf. Sci. 127–129 (1998) 71.
[25] I.W. Boyd, T.D. Binnie, J.I.B. Wilson, M.J. Colles, J. Appl. Phys. 55 (1984) 3061.
[26] S. Boughaba, X. Wu, E. Sacher, M. Meunier, in: Proceedings of the 19th Annual Meeting of Adhesion Society, Adhesion Society, Blacksburg, VA, 1996, p. 509.
[27] M.K. Shi, E. Sacher, M. Meunier, in: Proceedings of the 20th Annual Meeting of Adhesion Society, Adhesion Society, Blacksburg, VA, 1997, p. 385.
[28] http://www.srim.org/.
[29] J. Boussinesq, Comp. Rend. 114 (1892) 1510.
[30] S. Timoshenko, J.N. Goodier, Theory of Elasticity, second ed., McGraw-Hill, New York, 1951, p. 101.
[31] P.A. Engel, Impact Wear, Elsevier, New York, 1976, p. 42.
[32] M. Birnbaum, J. Appl. Phys. 36 (1965) 3688.
[33] J.F. Young, J.E. Sipe, J.S. Preston, H.M. van Driel, Phys. Rev. B 27 (1983) 1141;
J.F. Young, J.E. Sipe, J.S. Preston, H.M. van Driel, Phys. Rev. B 27 (1983) 1155;
J.F. Young, J.E. Sipe, J.S. Preston, H.M. van Driel, Phys. Rev. B 30 (1984) 2001.
[34] D. Bäuerle, Laser Processing and Chemistry, third ed., Springer-Verlag, Berlin, 2000 (Chapter 28).